ELSEVIER

Investigation of short-range nucleon-nucleon correlations using the reaction ^{12}C$(e,e'pp)$ in close to 4π geometry

K.I. Blomqvist [a], W.U. Boeglin [a], R. Böhm [a], M. Distler [a], R. Edelhoff [a,1],
J. Friedrich [a], R. Geiges [a], M.K. Jones [e], M. Kahrau [a], M. Korn [a], H. Kramer [a],
K.W. Krygier [a], V. Kunde [a], M. Kuss [b], A. Liesenfeld [a], K. Merle [a], C.L. Morris [c],
R. Neuhausen [a], E.A.J.M. Offermann [a], Th. Pospischil [a], M. Potokar [d],
R.D. Ransome [e], A.W. Richter [a], B.G. Ritchie [f], A. Rokavec [d], G. Rosner [a,2],
J. Ryckebusch [g], P. Sauer [a], S. Schardt [a], B. Vodenik [d], A. Wagner [a],
Th. Walcher [a], S. Wolf [a], M.K. Yadav [e]

[a] *Institut für Kernphysik, Johannes Gutenberg-Universität, J.J.-Becher-Weg 45, D-55099 Mainz, Germany*
[b] *Institut für Kernphysik, TH Darmstadt, D-64289 Darmstadt, Germany*
[c] *Physics Division, Los Alamos National Laboratory, Los Alamos, NM 87545, USA*
[d] *Institute Jožef Stefan, University of Ljubljana, Ljubljana, Slovenia*
[e] *Department of Physics and Astronomy, Rutgers University, Piscataway, NJ 08855-0849, USA*
[f] *Department of Physics and Astronomy, Arizona State Univ., Tempe, AZ, USA*
[g] *Department of Subatomic and Radiation Physics, Univ. of Gent, Proeftuinstraat 86, B-9000 Gent, Belgium*

Abstract

Two-proton correlations were studied in close to 4π geometry using the reaction ^{12}C$(e,e'pp)$. The beam energy was 705 MeV, the energy transfer 225 MeV, and the three-momentum transfer 412 MeV/c. The electrons were observed in a large-acceptance magnetic spectrometer in coincidence with protons observed in a BGO crystal ball. Missing energy and momentum, relative momentum and angular distributions were derived and compared with a factorized two-nucleon emission model. Soft-core correlation functions are favoured by the data. © 1998 Elsevier Science B.V.

PACS: 21.30.-x; 25.30.Fj; 24.50.+g; 27.20.+n
Keywords: Short-range nucleon-nucleon correlations

The phenomenological independent particle model (IPM) of the nucleus assumes that the mutual attraction of the nucleons averages to a mean nuclear field

in which pointlike nucleons move. Already in the 1940's Fermi realized that this conception is too naïve [1]. Without *repulsive* short-range forces between the nucleons any nucleus would just collapse to a size corresponding to the range of the attractive nuclear force (about 2 fm), even when Pauli-blocking is taken into account. In the IPM the nucleons are described by stationary states extending over the nuclear size (about 5 fm for ^{12}C). This means that a nucleon's mean free path is of the same order. The strong repulsive nucleon-nucleon interaction in the nuclear many body system needed to explain this quantum-gas like behaviour is related to the repulsive core seen in nucleon-nucleon (NN) scattering. Self-consistent Hartree-Fock calculations making use of the corresponding NN potentials do not describe nuclear properties correctly [2]. With the Bethe-Goldstone equation, on the other hand, the repulsive part of the NN potential can be accounted for [3,4]. The effects of this repulsion are usually referred to as short-range correlations (SRC).

It has been difficult to obtain a clear experimental signature of SRC in nuclei. Quasi-elastic ($e,e'p$) measurements gave indirect evidence for the presence of SRC. It was found that the occupation probabilities for the valence shells are considerably smaller than predicted by the IPM [5]. According to Refs. [6,7], part of the quasi-hole strength is shifted to high (missing) momenta, well above the Fermi momentum (about 220 MeV/c in carbon or oxygen), and high missing energies. At these energies, background processes like pion production and proton-neutron emission following the absorption of a virtual photon on meson exchange currents (MEC) might dominate the ($e,e'p$) cross section. This makes it hard to interpret the ($e,e'p$) data at high missing energies in terms of short-range correlations [8,9]. The ($e,e'p$) reaction is predicted to be rather insensitive to SRC at low missing energies [7]. Nonetheless, for missing momenta above 500 MeV/c low lying exited states in ^{15}N populated in the reaction $^{16}O(e,e'p)$ displayed a nucleon momentum density one order of magnitude larger than predicted by a mean field calculation [10]. For ($e,e'p$) reactions on the heavy target nucleus ^{208}Pb the surplus cross section at high missing momenta was attributed to long-range correlations [11].

It is more promising to go beyond ($e,e'p$) experiments and also observe the second (correlated) nucleon in two-nucleon ($e,e'NN$) knockout reactions, as first proposed by Gottfried [12]. In order to access small internucleon distances both nucleons should be in a state with large relative momentum. This one-body SRC process competes with two-body processes. Meson exchange currents and the excitation of the Δ resonance with a subsequent decay $\Delta N \rightarrow NN$ may also lead to the emission of two high energy nucleons. In order to suppress these background contributions we chose the reaction ($e,e'pp$) where MEC do not contribute to first (non-relativistic) order. Moreover, the contribution of the Δ resonance in the channel $pp \rightarrow \Delta^+ p \rightarrow pp$ is suppressed, if the two protons are initially in a relative S state (cf. Refs. [13,14]).

We performed inclusive (e,e') and exclusive ($e,e'p$) and ($e,e'pp$) measurements on ^{12}C for energy transfers ranging from below the quasi-elastic (QE) nucleon knockout up to and above the quasi-free excitation of the Δ resonance. This letter concentrates on the so-called ''dip'' region inbetween. The choice was made for three reasons. First, SRC are expected to play an important role in this energy transfer region. Calculations including only QE scattering, MEC and pion production underestimate the measured cross sections significantly [15]. Second, the probability of exciting the Δ should be kept small. Finally, the virtual photon must have enough energy to put two highly correlated nucleons onto the mass shell. This is difficult at the low energy side of the QE peak as one would need to sample very small cross sections at the required high momentum transfers. The photon should also have a large longitudinal polarization because it is the longitudinal nuclear response function that is predicted to exhibit a particularly large sensitivity to ground-state correlations [16,17]. SRC are expected to show a typical angular dependence [18]. It has not yet been determined by experiment which parts of the two-nucleon phase space $d\Omega_1 d\Omega_2 dT_1 dT_2$ are preferentially populated by short-range correlations. Therefore we investigated the reaction ^{12}C($e,e'pp$) within a large angular range, covering close to 4π in solid angle. Under restricted kinematics, this reaction has been measured before at NIKHEF [19].

The experiment was carried out at the electron scattering facility [20] at the 100% duty cycle Mainz

Microtron MAMI. The beam energy was 705 MeV, the beam current ranged from 30 to 300 nA. ^{12}C targets of 1 and 10 mg/cm^2 thickness were used. The luminosity was held constant at about 10^{33} nucleons $\cdot$ cm^{-2} $\cdot$ s^{-1}. The large acceptance, high resolution spectrometer A was positioned at a scattering angle of $\theta_{e'} = -34.5°$. The corresponding virtual photon's direction was $\theta_q = 41.3°$, its polarization $\varepsilon = 0.78$ ($\varepsilon = 1$ corresponds to maximum longitudinal polarization). The transferred four-momentum $Q = [\omega, |\boldsymbol{q}|]$ amounted to $[(225 \pm 55)\,\text{MeV}, (412 \pm 58)\,\text{MeV/c}]$.

The protons were detected in coincidence with the scattered electrons with the LAMPF BGO crystal ball surrounding the target. The BGO ball is described in [21]. The full ball consists of 30 equal solid angle detectors covering polar angles from 19° to 161°. For this experiment, two downstream detectors in the direction of the spectrometer were removed. These covered polar angles from 19° to about 60° and azimuthal angles from about 108° to 252°. The three remaining downstream detectors were moved out 3 cm to reduce the rate of low energy electrons, giving a forward angle limit of 26°. Each detector consists of a 5.6 cm thick BGO crystal with a 3 mm NE102A plastic scintillator optically coupled to the front face, allowing particle identification to be done as described in Ref. [21]. Each crystal was energy calibrated using the reaction $H(e, e'p)$. The calibration was monitored with a N$_2$ laser during the data taking. The energy resolution (FWHM) for a single detector was about 5% for proton kinetic energies up to 185 MeV at which energy the protons passed through the BGO crystal. The energy threshold for detecting protons was 30 MeV taking into account electronic thresholds and the material in front of the detector.

The low-energy electron background from atomic scattering processes was suppressed by a mini-orange mounted around the 1 cm wide beampipe right downstream of the target. The mini-orange consisted of six wedge-shaped NdFeB permanent magnets of 1.2 T magnetization. Each magnet covered polar angles from less than 19° to 90° and had an azimuthal angular width of 30°, thus covering one half of the solid angle for polar angles less than 90°. NE102A plastic scintillators of 3 mm thickness were mounted radially on top of each of the magnets in order to veto high energy protons or pions passing the magnet. The mini-orange decreased the background rate by a factor of 20 down to a maximum of 140 kHz per crystal. In total, the ball was operated at a singles count rate of 1.3 MHz above electronic threshold. The coincidence time resolution was 1 ns. The random coincidence rate in the proton exit channels was negligible.

The luminosity in the ^{12}C$(e, e'pp)$ experiment was determined from scaled down ^{12}C(e, e') singles, simultaneously accepted in spectrometer A. These were normalized to a set of precision inclusive (e, e') measurements taken under identical kinematic conditions. For these measurements, we used a high beam current of 31.2 μA and a target of well determined thickness (65 mg/cm^2). The beam current was measured on an absolute scale with a DC current transformer (Förster probe) to a precision of ± 100 nA. Since proton singles were not allowed to pass the trigger electronics, the computer deadtime could be kept below 10%. The data were corrected for the corresponding loss in count rate. The loss of protons via hadronic interactions in the material in front of the detectors and in the BGO crystals themselves was calculated and corrected for by using the program GEANT. It amounted to 5% at the most probable proton kinetic energy of 80 MeV for the proton-proton coincidences investigated in this paper. The missing energy spectra of the reaction ^{12}C$(e, e'pp)$ were corrected for radiative losses according to Ref. [22]. They amounted to less than 20% for missing energies up to 70 MeV. The $(e, e'pp)$ spectra were divided by the integrated luminosity and normalized bin by bin to the acceptance of the set-up, which was calculated with a Monte Carlo program. As a result, one obtains 9-fold differential cross sections. These cross sections subsequently were averaged over the (small) acceptance of the electron spectrometer and the (large) acceptance of the BGO crystal ball. The total systematic error of the cross sections is estimated to be 5%.

In Fig. 1, the average nine-fold differential cross section in the laboratory system is shown as a function of the missing energy defined as $E_m = \omega - T_1 - T_2 - T_{A-2}$, where $\omega = E_e - E_{e'}$ is the energy transfer, E_e is the incident electron energy, $E_{e'}$ is that of the scattered electron. T_1 and T_2 are the kinetic energies of the first and second proton, and
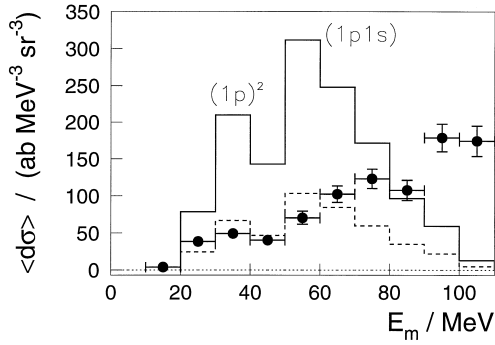
Fig. 1. Average nine-fold differential cross section $\langle d\sigma \rangle$ as a function of missing energy E_m. Cross section units are attobarns, $1\,ab = 10^{-46}\,m^2$. Dots denote data, horizontal bars the E_m integration interval, vertical bars the statistical error only. The histograms display calculations including either a hard-core (HC, solid line, Ref. [29]) or a soft-core correlation function (VMC, dashed line, Ref. [30]). The maxima are due to two-proton knock-out from the 1p shell and from the 1p and 1s shells, respectively.

T_{A-2} is the kinetic energy of the recoiling $(A-2)$ system ^{10}Be, calculated from the measured missing momentum $\boldsymbol{P}_m = \boldsymbol{q} - \boldsymbol{p}_1 - \boldsymbol{p}_2$, where $\boldsymbol{q} = \boldsymbol{p}_e - \boldsymbol{p}_{e'}$ is the 3-momentum transfer. $\boldsymbol{p}_e$, $\boldsymbol{p}_{e'}$, $\boldsymbol{p}_1$ and $\boldsymbol{p}_2$ are the momenta of the incident electron, the scattered electron and the two emitted protons, respectively. The recoil kinetic energy $T_{A-2} = p^2_{^{10}\mathrm{Be}}/(2\,m_{^{10}\mathrm{Be}})$ follows from $\boldsymbol{p}_{^{10}\mathrm{Be}} = \boldsymbol{P}_m$.

Fig. 1 also shows calculations that take into account nucleon-nucleon correlations and the excitation of the Δ resonance in a factorized ansatz for the $(e,e'pp)$ cross section according to Refs. [16,23]. Two main assumptions were made. First, a plane wave description of the outgoing protons was adopted. Second, it was assumed that the virtual photon couples to either one of the two protons and that the two protons resided in a relative S state. Then the 9-fold differential $(e,e'pp)$ cross section reads as

$$\frac{d^9\sigma}{d\omega\,d\Omega_{e'}\,dT_1\,d\Omega_1\,dT_2\,d\Omega_2}$$
$$= E_1\,p_1\,E_2\,p_2\,\sigma_{epp}\big(p^{(1)},p^{(2)},q\big)\,F_{h_1,h_2}\big(E_m,P_m\big)\,, \tag{1}$$

with the relative momenta per nucleon in the initial dinucleon system $p^{(1)} = |(\boldsymbol{p}_1 - \boldsymbol{q}) - \boldsymbol{p}_2|/2$ or $p^{(2)} = |\boldsymbol{p}_1 - (\boldsymbol{p}_2 - \boldsymbol{q})|/2$, depending on which one of the

two protons absorbed the virtual photon. E_1 and E_2 denote the total energies of the two emitted protons. $F_{h_1,h_2}(E_m,P_m)$ stands for the joint probability to find a pair of nucleons with momentum P_m in the single-particle states (h_1,h_2) at an energy corresponding to the missing energy. The momentum dependence of $F_{h_1,h_2}(E_m,P_m)$ is calculated within an harmonic oscillator model. The missing energy dependence was determined using the procedure outlined in Ref. [24]. The "elementary" cross section σ_{epp} describes the physics of the absorption of a virtual photon on a diproton embedded in the target nucleus. It depends on the photoabsorption mechanisms and on the relative motion of the two protons within the pair. As outlined in Ref. [16], σ_{epp} can be expressed as a sum of three terms containing longitudinal, transverse and transverse-transverse interference structure functions. These structure functions, in turn, depend on the nuclear one and two body current operators and on scalar (Jastrow), spin-spin, and tensor correlation operators. The latter two were considered only in the longitudinal channel. In Ref. [16], calculations within this model were compared with experiment [19] and unfactorized cross sections using either plane or distorted outgoing proton waves. It was shown, that the factorized ansatz gives a fair description of the ^{12}C$(e,e'pp)$ reaction in the dip region. Integrating the theoretical $(e,e'pN)$ cross section over the second nucleon N (mostly a neutron), one obtains ^{12}C$(e,e'p)$ cross sections [25] which also agree reasonably well with experimental ones in the dip [26,27] and Δ region [28].

The nine-fold differential cross section of Eq. (1) is used as input to an event-generator for the Monte Carlo program mentioned above. Thus, the simulated events are treated in exactly the same way as the data. Specifically, the averaging procedure is the same. In this way, a direct comparison of experimental and theoretical cross sections becomes possible. The central correlation functions used in our calculations fall into two groups, "hard-core" (HC) and "soft-core" (SC). An example for the first type is the 0.6 fm hard-core correlation function of Ref. [29]. The second category contains, first, state dependent correlation functions from the Argonne v_{14} potential applying variational Monte Carlo methods (VMC, Ref. [30]). Following the correlated basis function (CBF) approach, a second SC correlation function

was obtained in Ref. [31] from a systematic study of medium-heavy doubly closed shell nuclei using the Fermi hypernetted chain (FHNC) technique. In this calculation, the ground-state energy was minimized in the second order cluster expansion. Finally, a third SC correlation function (GM for G-matrix, Ref. [32]) is considered in this paper. It is the result of a self-consistent nuclear matter calculation that takes into account the effect of the nuclear medium on nucleon properties using Green's function methods. It was obtained from a comparison of the $^1S_0$ two-body density matrix elements describing the relative motion of dressed nucleons with and without interaction.

Fig. 1 shows that the calculation using the hard-core correlation function of Ref. [29] overestimates the data by a factor of 3 at small missing energies $E_m \leq 70\,\text{MeV}$ while the VMC correlation function reproduces the experimental cross sections reasonably well, as do the other two SC correlation functions FHNC and GM (not shown in the figure). Missing energies below $70\,\text{MeV}$ correspond to two-proton knockout from the 1p shell and from the 1p and 1s shells, as indicated in Fig. 1. The two-proton knockout from the 1s shell is calculated to lie at missing energies larger than $70\,\text{MeV}$. Its contribution to the cross section is small. It constitutes the shoulder of the calculated 1p1s peak in Fig. 1. We do not consider it here because of the growing contribution from other processes (three-nucleon emission) at those missing energies. This energy region will be addressed in a forthcoming paper.

The missing momentum distributions, shown in Fig. 2, are also better described by calculations using the SC correlation functions, with the HC cross sections being a factor 3 too large at small missing momenta $P_m < 0.5\,\text{GeV/c}$. The SC correlations only slightly overestimate the measured cross section in this missing momentum region for both $E_m \leq 50\,\text{MeV}$, corresponding mainly to two proton knockout from the 1p shell (upper panel of Fig. 2) and $E_m \leq 70\,\text{MeV}$ (lower panel of Fig. 2) which also includes knockout from the 1p and 1s shells.

In the present experiment, the high missing momentum region has been accessed for the first time in an $(e, e'pp)$ measurement. Interestingly, the data deviate strongly from the calculation for momenta above $P_m \approx 0.5\,\text{GeV/c}$, around $0.8\,\text{GeV/c}$ by about
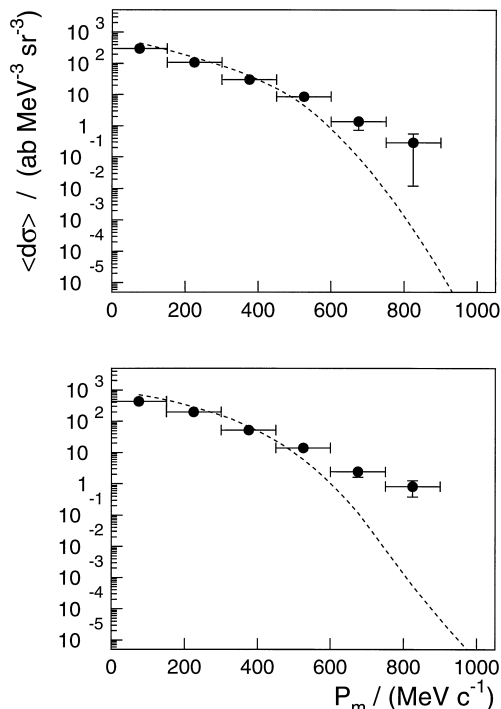

Fig. 2. Missing momentum P_m distribution for missing energies $E_m \leq 50\,\text{MeV}$ (upper panel) and $E_m \leq 70\,\text{MeV}$ (lower panel). The dashed curves display calculations using the soft-core variational Monte Carlo (VMC) correlation function of Ref. [30].

3 orders of magnitude. The experimental distribution strikingly resembles the two-nucleon momentum distribution [33] obtained from a so-called "lowest order approach" to multi-nucleon correlations in ^{16}O. This indicates that short-range correlations modify the pair momentum distribution at high momenta. Of course, the cross sections are very small at high P_m. Therefore, the bulk of the data is still well described by Eq. (1). Yet, the measurement of missing momenta up to very high values could be a new way to investigate the effect of short-range correlations in nucleon clusters comprising more than two nucleons.

One of the assumptions of the factorized model, used in this paper, is a plane wave description of the protons escaping from the residual nucleus. At first glance, this may seem to be too approximate. There is growing evidence, however, that final state interactions in electron or photon-induced two-nucleon knockout reactions are fairly small as long as low missing energies are considered. At these energies, it
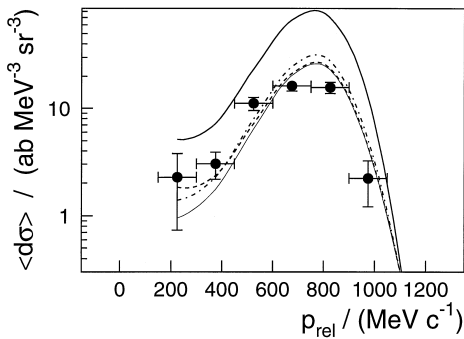
Fig. 3. Proton-proton relative momentum p_{rel} distribution for missing energies $E_m \leq 70\,\mathrm{MeV}$. The curves represent calculations including SRC according to Refs. [29] (HC, thick solid line), [30] (VMC, dashed line), and [32] (GM, dash-dotted line). The bottom thin solid curve was obtained under the assumption of no SRC. It represents the contribution of the Δ resonance.

is very probable that only two protons participate in the reaction process, as the missing momentum dependence of the $^{12}\mathrm{C}(e,e'pp)$ cross section clearly shows. Fig. 2 illustrates that the data essentially follow the proton pair distribution function $F_{h_1,h_2}(E_m, P_m)$ at $E_m \leq 70\,\mathrm{MeV}$ (except for very high missing momenta $P_m > 0.5\,\mathrm{GeV}/c$). A behaviour of this type was also observed in the $^{12}\mathrm{C}(\gamma,pp)$ reaction [34]. For both $^{12}\mathrm{C}(\gamma,pp)$ and $^{12}\mathrm{C}(\gamma,pn)$, differences of only about 20% were found in calculations with either plane or distorted outgoing nucleon waves [35]. As in the present experiment, the real photon studies address a situation in which the two nucleons are primarily emitted back-to-back and in which a large part of the phase space is covered.

The distribution of the proton-proton relative momentum is expected to be the quantity most sensitive to short-range correlations. Fig. 3 displays the distribution of the relative momentum $p_{rel} = |\boldsymbol{p}_1 - \boldsymbol{p}_2|$. Neglecting relativistic effects, this quantity equals the relative momentum in the centre-of-mass system of the two emitted protons. Relative momenta as high as $1\,\mathrm{GeV}/c$ were accessible. The $0.6\,\mathrm{fm}$ hard-core correlation function overestimates the data by up to half an order of magnitude for $p_{rel} > 600\,\mathrm{MeV}/c$. The soft-core VMC, GM and FHNC correlation functions also somewhat overestimate the experimental cross sections at $p_{rel} \approx 800\,\mathrm{MeV}/c$. The calculation using the FHNC correlation function gives nearly the same result as the VMC calculation

and is not shown in the figure. The data clearly favour the soft-core correlation functions, but do not discriminate between them. The main reason is the background from the $\Delta^+ p \rightarrow pp$ process (thin solid line in Fig. 3). Even when choosing the two-proton exit channel at a moderate energy transfer ω far from the Δ resonance peak, the Δ contribution to the cross section does not seem to be sufficiently suppressed.

Given that the excitation of the Δ resonance is predicted to be the origin of a considerable fraction of the detected $(e,e'pp)$ strength and taking into account that the $(e,e'pn)$ channel is likely to be stronger than its two-proton counterpart, one may wonder about the role of (n,p) rescattering possibly feeding the two-proton channel after the absorption of a virtual photon on a proton-neutron pair. Theoretical calculations [36] have shown that rescattering effects contribute little to the $(e,e'pp)$ cross section. The analysis of a $^{12}\mathrm{C}(\gamma,pp)$ experiment performed at low photon energies ($E_\gamma \leq 150\,\mathrm{MeV}$) [37] also supports the assumption that the charge-exchange contribution to two-proton knockout is small. Despite the fact that the ratio of pn to pp knockout at these small momentum transfers is large (typically 25), the shape and magnitude of the $^{12}\mathrm{C}(\gamma,pp)$ cross sections at low missing energies is consistent with direct knockout after photoabsorption on a diproton.
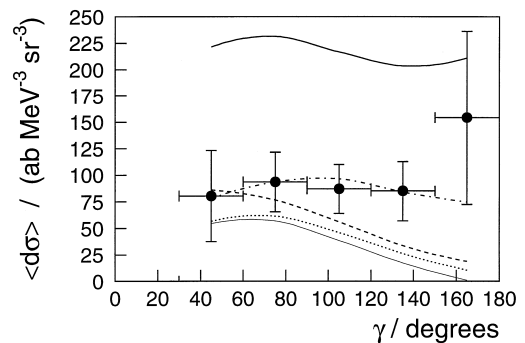

Fig. 4. Proton-proton angular correlation function for missing energies $E_m \leq 70\,\mathrm{MeV}$. γ denotes the angle between the two protons where one of the protons was emitted in the direction of the momentum transfer $\boldsymbol{q}$. The curves represent calculations using various SRC functions (see text): HC (thick solid line, Ref. [29]), GM (dash-dotted, Ref. [32]), VMC (dashed, Ref. [30]) and FHNC (dotted, Ref. [31]). The thin bottom curve was again obtained by turning off SRC (cf. Fig. 3).

The Δ contribution can be further suppressed by selecting protons where one of the two is emitted in the direction of the momentum transfer q. The angular correlation between these protons is shown in Fig. 4. Clearly, the contribution from isobaric currents is greatly reduced. This is particularly true in *super-parallel* kinematics where, in addition, the second proton is detected opposite to the first one ($\gamma = 180°$ in Fig. 4). Under these kinematic conditions, the contribution from resonant pion production is largely suppressed because the M_{1+} multipole dominates the excitation of the Δ in the pair and does not contribute at $\gamma = 180°$ if one disregards Fermi motion (see also Ref. [38]). Non-resonant π^0 production on a proton with subsequent reabsorption on another proton, a process not considered in our model, is expected to contribute little in the dip region.

Super-parallel kinematics also allow a Rosenbluth-type separation of the longitudinal and transverse part of the $(e,e'pp)$ cross section, as first pointed out in Ref. [18]. In this way, the longitudinal part of the $(e,e'pp)$ cross section, the most sensitive to SRC, becomes accessible. Therefore, these kinematics are an ideal choice for studying short-range NN correlations in more detail in future experiments. A pilot $(e,e'pp)$ experiment in super-parallel kinematics using three high resolution magnetic spectrometers was recently performed at MAMI.

The correlation function that reproduces the angular correlation best is the GM one (dash-dotted curve in Fig. 4) of Ref. [32]. It is not as soft as VMC and FHNC, for which the probability of finding two nucleons at zero relative distance in the nucleus is finite, whereas it approaches zero for the GM correlation function as the inter-nucleon distance tends to zero.

In summary, for the first time short-range nucleon-nucleon correlations were studied in electron-induced two-proton knockout reactions in close to 4π geometry. The energy transfer ω in the reaction $^{12}C(e,e'pp)$ was chosen to lie in the dip region. Missing energies corresponding to two-proton knockout from the 1p shell and the 1p and 1s shells were selected. The distributions of the missing (or pair) momentum and of the proton-proton relative momentum in the final state were measured up to $1\,GeV/c$. It was found that the largest sensitivity

with respect to different NN correlation functions appears in the proton-proton angular correlation around super-parallel kinematics. The data favour soft-core correlation functions, in particular the GM one, over the 0.6 fm hard-core correlation function.

References

[1] E. Fermi, Nuclear Physics, The University of Chicago Press, 1948, p. 111.
[2] K.A. Brueckner et al., Phys. Rev. 95 (1954) 217.
[3] H.A. Bethe, Phys. Rev. 103 (1956) 1353.
[4] J. Goldstone, Proc. Roy. Soc. (London) A 239 (1957) 267.
[5] L. Lapikás, Nucl. Phys. A 553 (1993) 297c.
[6] C. Mahaux, R. Sartor, Adv. Nucl. Phys. 20 (1991) 61.
[7] H. Müther, W.H. Dickhoff, Phys. Rev. C 49 (1994) R17.
[8] L.J.H.M. Kester et al., Phys. Lett. B 344 (1995) 79.
[9] J. Ryckebusch et al., Phys. Lett. B 350 (1995) 1.
[10] I. Blomqvist et al., Phys. Lett. B 344 (1995) 85.
[11] I. Bobeldijk et al., Phys. Rev. Lett. 73 (1994) 2684.
[12] K. Gottfried, Nucl. Phys. 5 (1958) 557.
[13] P. Wilhelm et al., Nucl. Phys. A 597 (1996) 613.
[14] C.J.G. Onderwater et al., Phys. Rev. Lett. 78 (1997) 4893.
[15] P. Barreau et al., Nucl. Phys. A 402 (1983) 515.
[16] J. Ryckebusch, Phys. Lett. B 383 (1996) 1.
[17] W.J.W. Geurts et al., Phys. Rev. C 54 (1996) 1144.
[18] C. Giusti, F.D. Pacati, Nucl. Phys. A 535 (1991) 573.
[19] L.J.H.M. Kester et al., Phys. Rev. Lett. 74 (1995) 1712.
[20] I. Blomqvist et al., accepted for publication in Nucl. Instr. and Meth. A (1997).
[21] R.D. Ransome et al., Phys. Rev. C 42 (1990) 1500.
[22] J.W.A. den Herder et al., Nucl. Phys. A 490 (1988) 507.
[23] M. Vanderhaeghen et al., Nucl. Phys. A 580 (1994) 551.
[24] J. Ryckebusch et al., Phys. Rev. C 49 (1994) 2704.
[25] J. Ryckebusch et al., Phys. Lett. B 333 (1994) 310; Nucl. Phys. A, 1997, in press.
[26] G.E. Cross et al., Nucl. Phys. A 593 (1995) 463.
[27] L.B. Weinstein et al., Phys. Rev. Lett. 64 (1990) 1646.
[28] H. Baghaei et al. Phys. Rev. C 39 (1989) 177.
[29] T. Ohmura et al., Prog. Theor. Phys. 15 (1956) 222.
[30] S.C. Pieper et al., Phys. Rev. C 46 (1992) 1741; private communication.
[31] F. Arias de Saavedra et al., Nucl. Phys. A 605 (1996) 359; private communication.

[32] C.C. Gearhart, Ph.D. thesis, Washington Univ., 1994, unpublished; W. Dickhoff, private communication.

[33] G. Orlandini, L. Sarra, Two-body knockout reactions and two-body momentum distributions, in: J. Ryckebusch, M. Waroquier (Eds.), Proc. Second Workshop on Electromagnetically Induced Two-nucleon Emission, Gent, May 1995, Universiteit Gent, 1995, p. 1; private communication.

[34] P.D. Harty et al., Phys. Lett. B 380 (1996) 247.

[35] G.E. Cross et al., Nucl. Phys. A 593 (1995) 463.

[36] C. Giusti, F.D. Pacati, Nucl. Phys. A 585 (1995) 618.

[37] J.C. McGeorge et al., Phys. Rev. C 51 (1995) 1967.

[38] B. Körfgen et al., Phys. Rev. C 50 (1994) 1637